

Characteristic Angles in the Wetting of a Wedge-Shaped Region

Yuri O. Popov* Thomas A. Witten

*Department of Physics, University of Chicago,
5640 S. Ellis Ave., Chicago, IL 60637*

Abstract

The shape of a liquid surface bounded by an acute or obtuse wedge is considered by using classical analysis methods. For acute wedges the two principal curvatures are of the order of the (fixed) mean curvature. But for obtuse wedges, the principal curvatures both diverge as the vertex is approached. The power-law divergence becomes stronger with increasing opening angle. Possible implications of this contrasting behavior are suggested.

PACS: 68.03.Cd — Surface tension and related phenomena

1 Introduction

The shape of the surface of a liquid or soap film constrained at its boundaries is a classic subject of mathematical physics [1, 2, 3]. These studies demonstrate the power of producing very smooth surfaces of controlled curvature by choosing the shape of the boundary. The chief emphasis of these prior studies is to determine the global shape of the surface bounded by a given smooth surface. Here we emphasize the complementary question of the local surface shape in response to a singular boundary shape: namely, a line with a sharp bend enclosing a wedge-shaped droplet spanning an angle α . The role of singularities in governing the shape and the motion of fluids has aroused great current interest. Such singularities occur when a fluid droplet breaks apart [4, 5, 6, 7], when it merges another droplet [8, 9, 7], when it moves across a surface [10, 11, 12, 13, 14, 15, 16, 17], or when it moves through another fluid [18, 19, 20, 6].

Surprisingly, a qualitative change in the surface shape occurs as the opening angle of the boundary α increases past a right angle, as we show below. The curvatures for acute angles remain finite for the region near the vertex. But for obtuse angles, the curvatures diverge as the vertex is approached, with a power law that varies continuously with the angle.

*Corresponding author. E-mail: yopov@midway.uchicago.edu

Our motivation for focusing on wedge-shaped droplets arises from observations of irregular droplets seen in everyday life. These often have wedge-shaped regions arising from the vagaries of deposition and substrate shape. We have noticed that evaporation in these regions leads to distinctive drying patterns of solids dissolved in the liquid. To understand the nature of these drying patterns requires knowledge of the surface shape. For the circular drops the problem of the surface shape assumes very simple solution (spherical cap), allowing one to proceed with the issue of evaporation profiles up to the level of successful comparison of the theoretical results with the experimental data. This so called “coffee-drop deposits” problem has a number of possible applications and finds an extensive account in modern studies [21, 22, 23].

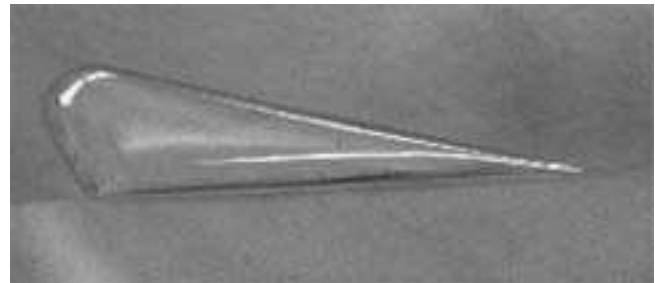
Specifically, we consider a droplet on the horizontal surface bounded by an angle α in the plane of the substrate (Fig. 1). We assume that the droplet is sufficiently small so that the surface tension is dominant, and the gravitational effects can be safely neglected (significance of gravity increases with the size of the drop). At the same time, we do *not* assume that the contact angle between the “liquid–gas” surface and the plane is constant along the boundary line on the substrate. To achieve a wedge shaped boundary, the substrate must have scratches, grooves or other inhomogeneities (sufficiently small comparing to the dimensions of the droplet), which *pin* the contact line. A strongly pinned contact line can sustain a wide range of contact angles; the angle is not fixed by the interfacial tensions as it is on a uniform surface (Fig. 2).

In the following section we first give a simple account of the shape that assumes that the liquid surface is nearly horizontal, and then we make a more systematic asymptotic analysis of the region where the distance r from the vertex is much smaller than the fixed inverse mean curvature R of the droplet, *not* making any *a priori* assumptions about the horizontalness of the surface. In the discussion section that follows, we calculate the curvatures of the obtained surface shape and describe some possible implications. In particular we discuss how the refraction of the light in the drop shows contrasting properties in acute versus obtuse wedges.

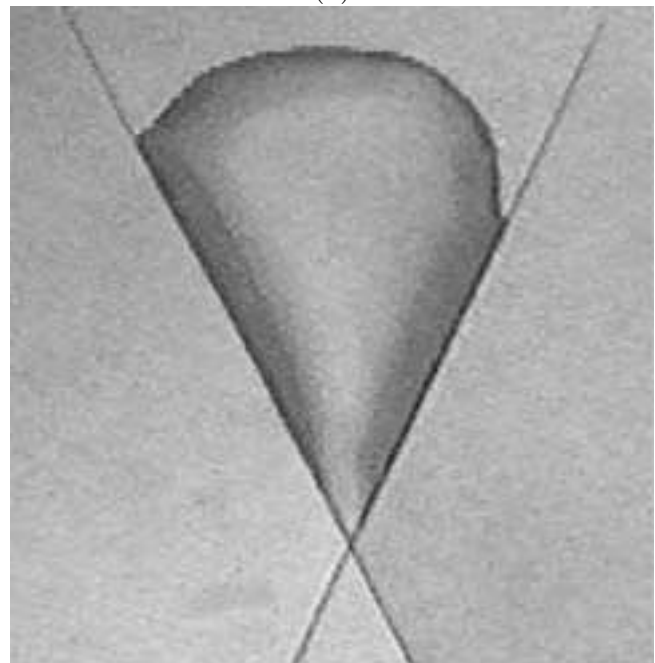
2 Calculation

Our purpose is to calculate the shape of the surface of the drop $z(r, \phi)$. Use of the cylindrical coordinates looks most natural in this problem so that the angle occupied by the liquid on the substrate is $0 < r < \infty$ and $-\alpha/2 < \phi < \alpha/2$ and hence the boundary conditions are $z(0, \phi) = z(r, -\alpha/2) = z(r, \alpha/2) = 0$. The surface shape $z(r, \phi)$ is that which minimizes the surface area $A = \iint [1 + (z'_r)^2 + (z'_\phi/r)^2]^{1/2} r dr d\phi$ (and hence the surface energy σA) while the volume of the liquid beneath the surface $V = \iint z r dr d\phi$ is kept fixed¹. This is equivalent to the minimization of the functional $A - \lambda V$ with respect to arbitrary variations of $z(r, \phi)$ that leave the boundary fixed, with λ being a Lagrange multiplier. The proper choice of this parameter is $\lambda = \Delta p/\sigma$, which arises from the expression for the total energy

¹The integrations are over the region occupied by the drop.



(a)



(b)

Figure 1: (a) Wedge-shaped water droplet on the substrate. (b) The same droplet pictured from another point of view. Black lines are the grooves on the substrate necessary to “pin” the contact line. (Photos by Itai Cohen.)

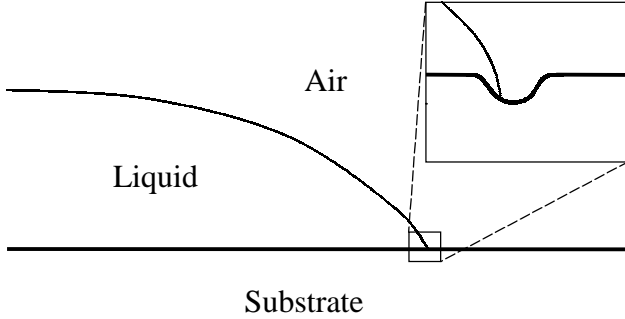


Figure 2: Illustration of the possibility of a wide range of contact angles in the presence of a groove or another inhomogeneity.

$E = \sigma A - \Delta p V$. Here σ is the surface tension and Δp is the pressure difference between liquid and gas ($\Delta p > 0$). Since we neglect the effects of gravity, the pressure within the droplet is constant, and so is Δp . Thus $\Delta p/\sigma$ is just a constant parameter of the dimensions of $1/\text{length}$. Since this is the only dimensional scale in the problem, introduction of the dimensionless variables $r/R \rightarrow r$ and $z/R \rightarrow z$ (where $R \equiv \sigma/\Delta p$) makes the mathematical formulation parameterless, resulting, in particular, in the choice $\lambda = 1$. Thereby we agree to measure all quantities of the dimension of length in units of R . Having found $z(r, \phi)$, one can restore the sought surface shape in ordinary units by simple substitution $z(r, \phi) \rightarrow Rz(r/R, \phi)$.

The Euler-Lagrange equation for the functional $A - \lambda V$ gives a second-order non-linear differential equation for the function $z(r, \phi)$:

$$\begin{aligned} & \left[z''_{\phi\phi} + rz'_r + r^2 z''_{rr} + \left\{ z''_{\phi\phi}(z'_r)^2 + r(z'_r)^3 + z''_{rr}(z'_\phi)^2 - 2z''_{r\phi}z'_rz'_\phi + 2z'_r(z'_\phi)^2/r \right\} \right] + \\ & + r^2 \left[1 + \left\{ (z'_r)^2 + (z'_\phi/r)^2 \right\} \right]^{3/2} = 0 \end{aligned} \quad (1)$$

Note that this equation could also have been obtained if we started from the Laplace equation for the surface tension:

$$2H = -\frac{\Delta p}{\sigma} \quad (\text{ordinary units}) \quad (2)$$

or

$$2H = -1 \quad (\text{dimensionless units}), \quad (3)$$

where H is the mean curvature of the surface $H = (c_1 + c_2)/2$ and c_1 and c_2 are the two principal curvatures. Given a surface $z(r, \phi)$, its mean curvature can be computed in terms of the coefficients of the first and the second fundamental quadratic forms of the surface, leading to the same eq. (1) (for a concise review of these results of the differential geometry see [24] or [1]).

Naive solution. There is no generic method for solving second-order non-linear differential equations of the kind of eq. (1), so we seek an approximate solution. First of all, we notice that if all derivatives of z are small ($z'_r \ll 1$ and $z'_\phi/r \ll 1$), i.e. if the surface is nearly

horizontal, then the curly brackets in each pair of the square brackets can be neglected with respect to the rest of the terms. Thus, an easy-to-solve Poisson equation is recovered:

$$\nabla^2 z = -1 \quad (4)$$

The general solution to this equation (going to 0 as $r \rightarrow 0$ in cylindrical coordinates) is well known:

$$z(r, \phi) = r^2 (A \cos 2\phi + B \sin 2\phi - 1/4) + \sum_{\nu} r^{\nu} (C_{\nu} \cos \nu\phi + D_{\nu} \sin \nu\phi) \quad (5)$$

Symmetry arguments yield $B = D_{\nu} = 0$, and boundary conditions $z(r, -\alpha/2) = z(r, \alpha/2) = 0$ lead to the final expression:

$$z(r, \phi) = \frac{1}{4} r^2 \left(\frac{\cos 2\phi}{\cos \alpha} - 1 \right) + C r^{\pi/\alpha} \cos \frac{\pi \phi}{\alpha} \quad (6)$$

The coefficient C depends on the total volume of the liquid in the drop and on the angle α . This simple solution works well in the full range² of values of angle α from 0 to π except for $\alpha = \pi/2$ where the first term has a singularity of $1/\cos \alpha$. Note that exactly this value separates the regions of dominance of the two terms in the limit $r \ll 1$: for $\alpha < \pi/2$ the r^2 -term dominates, while for $\alpha > \pi/2$ the $r^{\pi/\alpha}$ -term does. At $\alpha = \pi/2$ both terms scale with r as r^2 . This fact and an observation that there are no restrictions imposed on the dependence $C(\alpha)$ by the equation or by the boundary conditions suggest a way to cure the situation of the diverging coefficient $1/\cos \alpha$: In order to cancel this unphysical divergence, $C(\alpha)$ *must* have exactly the same singularity at $\alpha = \pi/2$ but of the opposite sign. Namely, let us consider α in the vicinity of $\pi/2$, i.e. let $\alpha = \pi/2 + \varepsilon$, where $|\varepsilon| \ll 1$. Then $z(r, \phi)$ (eq. (6)) becomes

$$\begin{aligned} z(r, \phi) = & \frac{1}{4} r^2 \left(-\frac{\cos 2\phi}{\varepsilon} (1 + O(\varepsilon^2)) - 1 \right) + \\ & + C(\varepsilon) r^2 \left(1 - \frac{4}{\pi} \varepsilon \ln r + O(\varepsilon^2) \right) \left(\cos 2\phi + \frac{4}{\pi} \varepsilon \phi \sin 2\phi + O(\varepsilon^2) \right) \end{aligned} \quad (7)$$

and it can remain finite as $\varepsilon \rightarrow 0$ only if function $C(\varepsilon)$ has a simple pole of the opposite sign at 0, i.e. if

$$C(\varepsilon) = \frac{1}{4\varepsilon} + C_0 + O(\varepsilon) \quad (8)$$

where C_0 is independent of ε . In this case the two terms of the order of $1/\varepsilon$ cancel, and one obtains a quite pleasing result in the vicinity of the right angle:

$$z(r, \phi) = -\frac{1}{\pi} r^2 \ln r \cos 2\phi + r^2 \left(\frac{1}{\pi} \phi \sin 2\phi - \frac{1}{4} + C_0 \cos 2\phi \right) + O(\varepsilon) \quad (9)$$

²Solution (6) cannot be used for $\alpha > \pi$ since in that range it violates the horizontalness requirement employed in its derivation.

Now, the main asymptotic in r is $(-r^2 \ln r)$ instead of expected r^2 . This is a rather typical situation for a power series solution near a crossover of two powers. Note also that derivation suggests the following domain of validity of result (9):

$$|\varepsilon \ln r| \ll 1 \quad \text{or} \quad e^{-1/|\varepsilon|} \ll r \ll e^{1/|\varepsilon|} \quad (10)$$

which can be realized only if $|\varepsilon| \ll 1$. Hence expansion (9) works the best at $\alpha = \pi/2$ and in the immediate vicinity of this value but nowhere else.

Asymptotic analysis. The results above required the assumption that the drop is nearly horizontal. This assumption has not been justified yet, and now we justify it via a more systematic treatment. Since we are interested in the behavior of the surface *near* the vertex of the angle, we introduce a new small parameter for the problem

$$r \ll R = \frac{\sigma}{\Delta p} \quad \text{(ordinary units)} \quad (11)$$

or

$$r \ll 1 \quad \text{(dimensionless units)} \quad (12)$$

For small r we may write $z(r, \phi)$ as a standard series expansion:

$$z(r, \phi) = r^\nu \Phi_\nu(\phi) + r^\mu \Phi_\mu(\phi) + \dots \quad (13)$$

where $0 < \nu < \mu < \dots$. Note that we do not restrict our attention to the horizontal case only, i.e. we do not require $1 < \nu$. All possible “not horizontal” values of ν between 0 and 1 will be eliminated automatically by application of boundary conditions to the solutions of eq. (1), proving thereby assumptions of the naive approach. Here we find only the main asymptotic (ν -term) and the first order correction (μ -term), but the method allows one to proceed up to an arbitrary order. Details of the calculation are considered in the Appendix; results are presented below. We also treat the case of the right angle separately since we expect logarithmic corrections to the main power of r and failure of the assumption (13).

Leading asymptotic. Substitution of $z(r, \phi) = r^\nu \Phi_\nu(\phi)$ into eq. (1) and retention of only the dominant terms for $r \ll 1$ lead to different equations for different possible values of power ν . Solution of those equations and application of symmetry arguments and boundary conditions eliminate some values of ν , leaving at the end only two possibilities ($\nu = 2$ and $\nu = \pi/\alpha$). For these two values the terms retained are a subset of those constituting eq. (4), yielding the following main order result:

$$z(r, \phi) = \begin{cases} \frac{1}{4} r^2 \left(\frac{\cos 2\phi}{\cos \alpha} - 1 \right) & \text{if } 0 \leq \alpha < \frac{\pi}{2} \quad (\nu = 2) \\ Cr^{\pi/\alpha} \cos \frac{\pi\phi}{\alpha} & \text{if } \frac{\pi}{2} < \alpha \leq \pi \quad (\nu = \pi/\alpha) \end{cases} \quad (14)$$

This agrees with the leading behavior of the naive solution (6) as $r \rightarrow 0$. Thus, our surface is indeed nearly horizontal, and the naive approach indeed produced a sensible result.

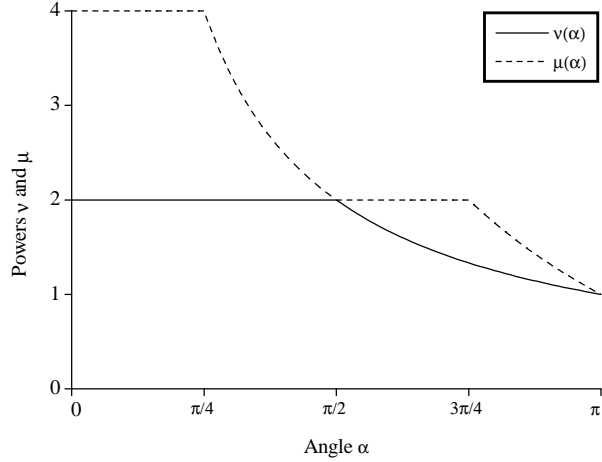


Figure 3: Dependences $\nu(\alpha)$ and $\mu(\alpha)$.

The constant C is again restricted by neither the equation nor the side boundary conditions. It is evidently determined by the bulk of the drop far from the vertex and may depend on α . As we will show below, the presence of an arbitrary constant C in the solution for obtuse angles is a direct result of a different asymptotic in r .

Dependence $\nu(\alpha)$ is shown on Fig. 3: for acute angles $\nu = 2$ and for obtuse ones $\nu = \pi/\alpha$.

First order correction. The final first-order result for the surface shape in the limit $r \ll 1$:

1. If $0 < \alpha < \pi/4$, then $\nu = 2$, $\mu = 4$ and

$$z(r, \phi) = \frac{1}{4}r^2 \left(\frac{\cos 2\phi}{\cos \alpha} - 1 \right) + \frac{1}{192}r^4 \left(\left[4\tan^2 \alpha - 3 \right] \frac{\cos 4\phi}{\cos 2\alpha} + \left[2\tan^2 \alpha + 12 \right] \frac{\cos 2\phi}{\cos \alpha} - \left[6\tan^2 \alpha + 9 \right] \right) + \dots \quad (15)$$

2. If $\pi/4 < \alpha < \pi/2$, then $\nu = 2$, $\mu = \pi/\alpha$ and

$$z(r, \phi) = \frac{1}{4}r^2 \left(\frac{\cos 2\phi}{\cos \alpha} - 1 \right) + Cr^{\pi/\alpha} \cos \frac{\pi\phi}{\alpha} + \dots \quad (16)$$

3. If $\pi/2 < \alpha < 3\pi/4$, then $\nu = \pi/\alpha$, $\mu = 2$ and

$$z(r, \phi) = Cr^{\pi/\alpha} \cos \frac{\pi\phi}{\alpha} + \frac{1}{4}r^2 \left(\frac{\cos 2\phi}{\cos \alpha} - 1 \right) + \dots \quad (17)$$

4. If $3\pi/4 < \alpha < \pi$, then $\nu = \pi/\alpha$, $\mu = 3\pi/\alpha - 2$ and

$$z(r, \phi) = Cr^{\pi/\alpha} \cos \frac{\pi\phi}{\alpha} + C^3 \frac{\pi^3}{4\alpha^2(2\pi - \alpha)} r^{(3\pi/\alpha)-2} \cos \frac{\pi\phi}{\alpha} + \dots \quad (18)$$

The structure of the solution (15)-(18) becomes clear if one plots functions $\nu(\alpha)$ and $\mu(\alpha)$ together (Fig. 3). Four powers of r appear in these formulas: r^2 , r^4 , $r^{\pi/\alpha}$ and $r^{(3\pi/\alpha)-2}$. For any given α our procedure selects the two lowest powers in this set of four. Different powers get selected for different α ; this leads to the four cases appearing in (15)-(18). In a full expansion, we expect *all* four powers to be present for all angles³. Indeed, the intermediate steps of the construction of the first two terms in the expansion of $z(r, \phi)$ allow us to predict the total structure of the full series: Two sets of additive terms constitute the solution. One set is the terms which are only the constant powers of r (2, 4, ...) and which have no free parameters dependent on the total amount of liquid (like C). The other set is the terms which do contain an arbitrary constant C and which are the hyperbolic powers of r (π/α , $(3\pi/\alpha) - 2$, ...). Since $Dr \cos \phi$ is the *exact* solution to the equation (1) when the boundary of the surface is a straight line $\alpha = \pi$, these hyperbolic powers of r all converge to unity as $\alpha \rightarrow \pi$.

Right-angle wedge: first two terms in the expansion. We already know that pure power series does not work in the case $\alpha = \pi/2$ and that the leading power of r should be close to 2, at most logarithmically close. So, we introduce a new *ansatz* instead of series (13):

$$z(r, \phi) = (-r^2 \ln r) \Phi_1(\phi) + r^2 \Phi_2(\phi) + \dots \quad (19)$$

Subsequently, by repeating the steps of the Appendix, we find $\Phi_1(\phi) = A \cos 2\phi$, then obtain the second term ($\Phi_2(\phi)$) and fix $A = 1/\pi$ by boundary conditions. As a result we recover expression (9):

$$z(r, \phi) = -\frac{1}{\pi} r^2 \ln r \cos 2\phi + r^2 \left(\frac{1}{\pi} \phi \sin 2\phi - \frac{1}{4} + C_0 \cos 2\phi \right) \quad (20)$$

where C_0 is a constant. Formula (20) is strictly valid as $r \rightarrow 0$ only for $\alpha = \pi/2$. For $\alpha \approx \pi/2$ it approximately holds for r small but nonzero. Expression (10) shows the regime of validity of this result. For any given small (but nonzero) r the validity domain is a vicinity ε of $\alpha = \pi/2$; for $r \rightarrow 0$ this domain is only one point — the right angle itself.

Thus, an asymptotic expansion of the dimensionless function z of dimensionless coordinates r and ϕ in the limit $r \ll 1$ has been found for all values of α in the range from 0 to π . A natural extension of this study is to consider wedges that are with $\alpha > \pi$. We guess that for such cases $z(r, \phi)$ grows as a power of r less than unity, so that the slope of the surface diverges at the vertex. But we have not succeeded to verify this behavior with our methods.

³Note that all terms satisfy boundary conditions independently.

Typical behavior of the universal function $z(r, \phi)$ (eqs. (15)-(18) and (20)) for angles $\alpha = 3\pi/8, \pi/2$ and $5\pi/8$ is shown on Fig. 4. To facilitate the comparison, we also plot the bisector cross sections of the three surface profiles in one frame (Fig. 5). Constant C_0 is taken to be 1 in all cases, while the value of constant C is chosen according to prescription (8).

3 Discussion

Curvature. Let us understand the main order result further by looking at the curvature of the surfaces described above. The principal curvatures along the bisector of the wedge are in the \hat{r} and $\hat{\phi}$ directions. For small r , the radial (c_{rr}) and the azimuthal ($c_{\phi\phi}$) curvatures are simply

$$c_{rr} = z''_{rr} \quad \text{and} \quad c_{\phi\phi} = \frac{z''_{\phi\phi}}{r^2} + \frac{z'_r}{r} \quad (21)$$

For an arbitrary point on the surface the two principal curvatures can also be determined from the coefficients of the first and the second fundamental quadratic forms of the surface (see [1, 24] for details). By either of these two methods, the principal curvatures on the bisector for the surface (14) and (20) are (up to the leading order in $r \ll 1$ only):

$$\begin{aligned} c_{rr} &= -\frac{1}{2} + \frac{1}{2 \cos \alpha} & c_{\phi\phi} &= -\frac{1}{2} - \frac{1}{2 \cos \alpha} & \text{if } 0 \leq \alpha < \pi/2 \\ c_{rr} &= -\frac{2}{\pi} \ln r & c_{\phi\phi} &= \frac{2}{\pi} \ln r & \text{if } \alpha = \pi/2 \\ c_{rr} &= C \frac{\pi(\pi-\alpha)}{\alpha^2} r^{(\pi/\alpha)-2} & c_{\phi\phi} &= -C \frac{\pi(\pi-\alpha)}{\alpha^2} r^{(\pi/\alpha)-2} & \text{if } \pi/2 < \alpha \leq \pi \end{aligned} \quad (22)$$

Typical behavior of radial curvature c_{rr} on the bisector as a function of r is shown on Fig. 6 for the same three values of α as on Figs. 4 and 5. Now the dramatic difference between the two regimes of α becomes apparent. For acute angles the curvatures remain finite as $r \rightarrow 0$ while for obtuse ones the curvatures diverge as a negative power of r (changing from 0 to -1 as angle α passes from $\pi/2$ to π). The limiting case of the right angle has an intermediate logarithmic divergence. Note that the finite values of curvature (for $\alpha < \pi/2$) sum to -1 in full accord with equation (3). However, the divergent values (for $\alpha \geq \pi/2$) have the opposite signs and thus sum to 0. This is a result of the neglect of the corrections to the main asymptotic in r . Dropping these corrections one should also drop -1 in the right hand side of eq. (3) to operate with quantities of the same order of magnitude. Had we kept the corrections to the divergent curvatures, they would sum to -1 . Thus, for instance, the second term in the solution (17) is the kind of the correction which provides summation to -1 when the main (divergent) terms sum to 0.

The origin of the arbitrary constant C in the solution (14) can now be easily understood. The pressure term in the Laplace equation (which is -1 in the dimensionless units) is what forces the prefactors to get fixed by its presence in the right hand side of the equation. Since this term matters only when the curvatures are finite, it does its job well for acute angles. When the curvatures diverge, the finite pressure term can not keep control over prefactors to “infinite” terms, and thus the arbitrariness of C arises in the cases of obtuse

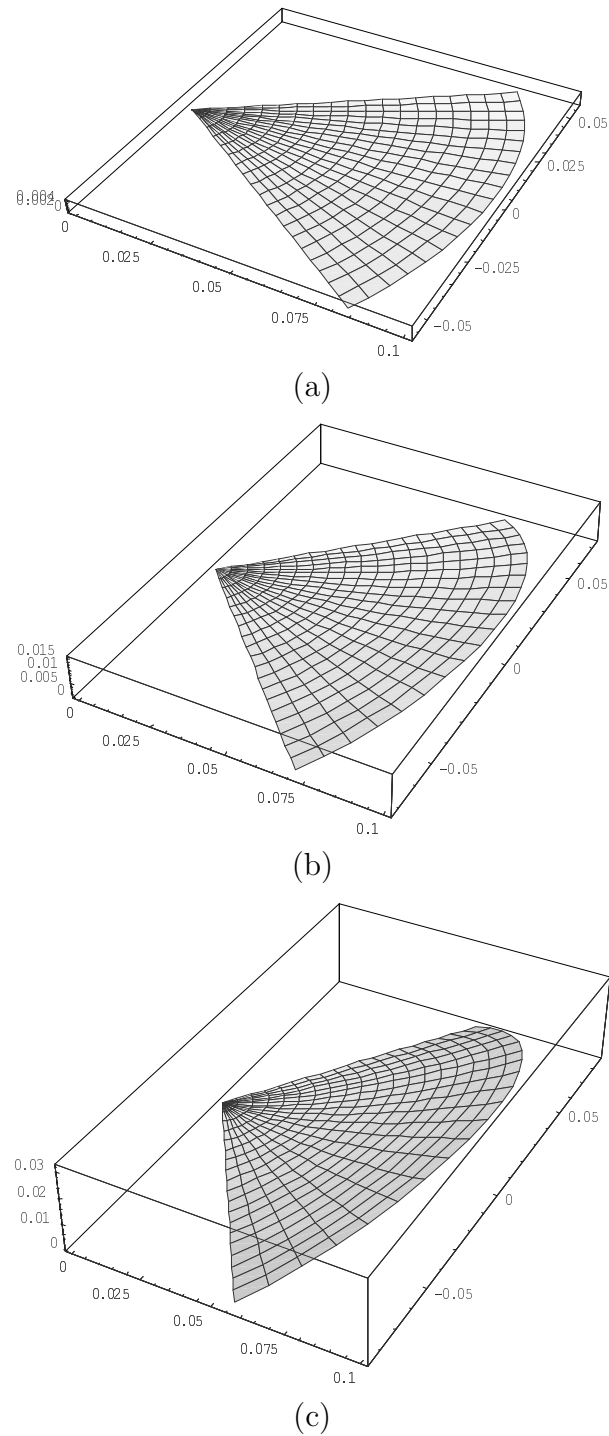


Figure 4: Surface shape $z(r, \phi)$ (first two terms of the expansion in r with $C = 1/(4\alpha - 2\pi) + C_0$ and $C_0 = 1$) for (a) $\alpha = 3\pi/8$ (eq. (16)), (b) $\alpha = \pi/2$ (eq. (20)), and (c) $\alpha = 5\pi/8$ (eq. (17)). The mathematical differences in the shapes are not apparent in this view.

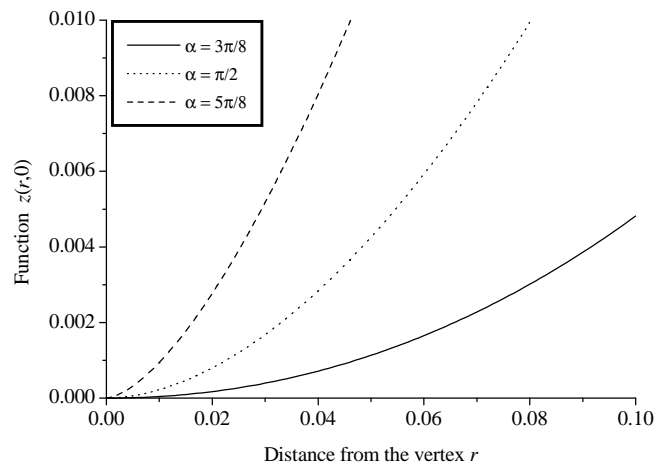


Figure 5: Surface profiles at bisector ($\phi = 0$) for three values of angle α .

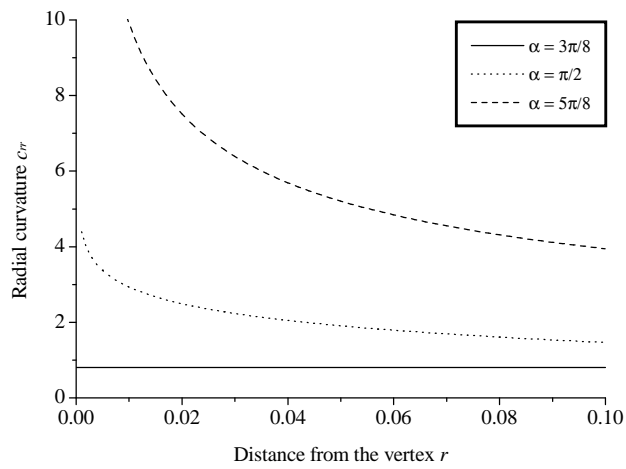


Figure 6: Radial curvature on the bisector for three values of angle α (main asymptotic only).

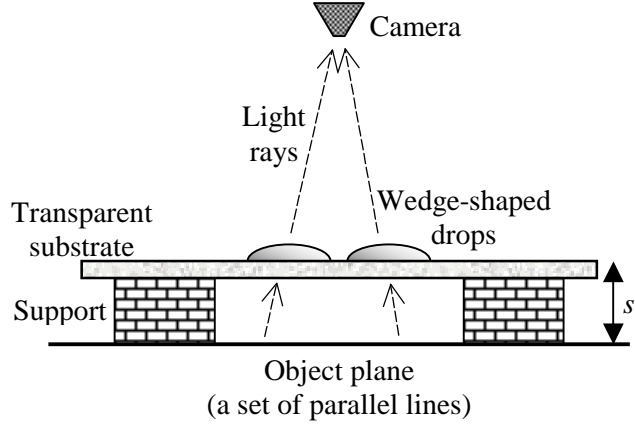


Figure 7: Experimental setup for the refraction demonstration.

and right angles. So, the r -dependence of the solution results in the presence or absence of undetermined coefficients in that solution.

Experimental realizations. The contrast between acute and obtuse wedges may be seen in the way they refract light. To illustrate, we picture a pair of wedge shaped droplets on a transparent substrate at a distance s above an object plane (Fig. 7). One wedge is acute, and the other one is obtuse. The object plane consists of a set of closely spaced parallel lines perpendicular to the bisectors of each wedge, so that the spacing between the lines is in the \hat{r} direction along the bisector. Observation of the object plane through the droplets allows one to make qualitative judgment about the behavior of the curvature near the vertices of each wedge. The result of such a simple demonstration with spacing between the parallel lines of approximately 1.6 mm, acute angle of about 51° , and obtuse angle of about 124° is shown in Figure 8. As it is apparent from this image, the spacing between the lines seen through the obtuse wedge *decreases* as they approach the vertex, while the spacing between the lines seen through the acute wedge remains unchanged. Note that only a few millimeters near the vertex should be taken into account while viewing this figure since the inverse mean curvature R for water drops not distorted by gravity is of this order of magnitude. At higher distances gravitational effects cannot be neglected while calculating the surface shape.

This observation agrees favorably to the result of our calculation, as it can be seen from an argument based on geometrical optics. Indeed, for the dimensions of the optical image along the bisector only radial curvature is important, and one can write the following approximate expression for the linear magnification by the drop in the \hat{r} direction:

$$m = \frac{1}{1 + s(n - 1)c_{rr}} \quad (23)$$

where n is the index of refraction of the liquid the droplets are made of⁴. According to our result, for obtuse wedges the curvature diverges and the magnification should go to zero as

⁴This expression assumes the horizontalness of the drop.

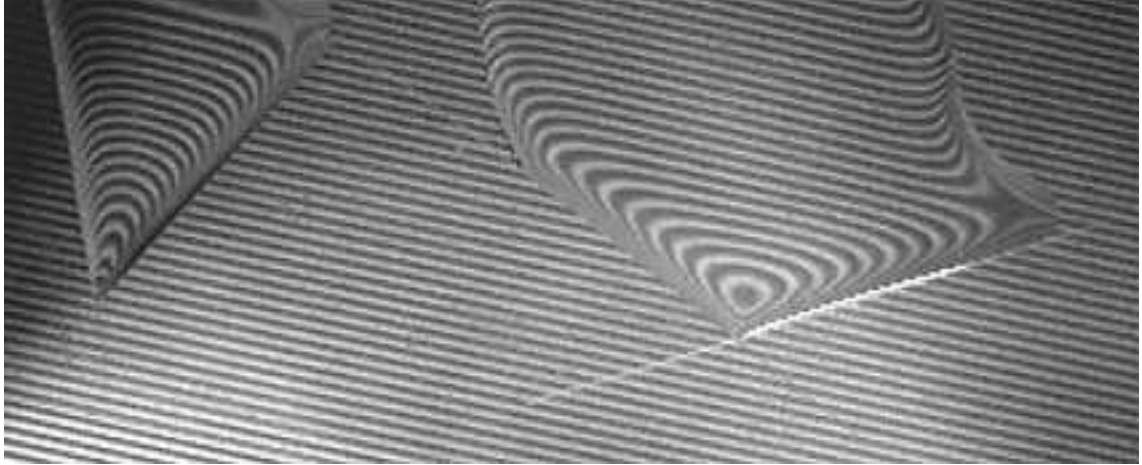


Figure 8: A set of parallel lines as seen through acute and obtuse wedges. The spacing between the undistorted lines is about 1.6 mm. The opening angles of the acute and obtuse wedges are approximately 51° and 124° respectively. (Photo by Itai Cohen.)

the vertex is approached; for acute angles both quantities remain finite. Thus, qualitative validity of our result is confirmed by the simple demonstration described above. Similar behavior should hold for the light reflected off the surface of the droplet because curvature is equally important for both such phenomena.

Another possible system to test the predictions of our study is a pressurized soap film. As shown in Figure 9, a soap film on a wedge-shaped frame with an applied constant pressure difference across it will have constant mean curvature. Thus, it is described by our formalism. The only difference between such a film and a liquid drop is that the film has two surfaces, and therefore the applied Δp must be two times as much as Δp in equation (2). Once such a surface is produced, it can be made as big as necessary for experimental convenience, since gravitational effects are virtually absent for this realization.

As these examples illustrate, the change in behavior on going from acute to obtuse wedges can show up in concrete ways. We suspect that further differences will emerge as capillary flow and evaporation properties of these wedge shaped liquid interfaces are explored.

The authors are grateful to Leo Kadanoff for an insightful discussion and to Itai Cohen for his help with photographing the drops. This work was supported in part by the MRSEC Program of the National Science Foundation under Award Number DMR-9808595.

Appendix

Here we present some details on how we obtain expressions (14) and (15)-(18). One starts from the substitution of $z(r, \phi) = r^\nu \Phi_\nu(\phi)$ (the first term of the expansion (13)) into eq. (1)

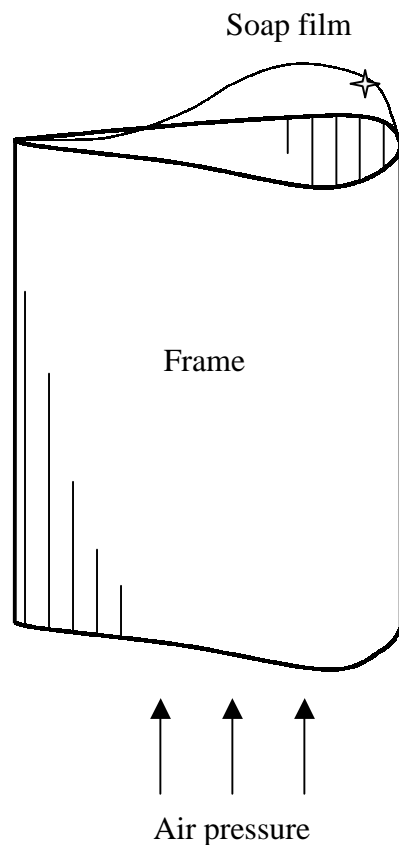


Figure 9: Pressurized soap film realization.

and obtains the following equation for $\Phi_\nu(\phi)$:

$$r^\nu \left(P[\Phi_\nu] + r^{2\nu-2} Q[\Phi_\nu] \right) + r^2 \left(1 + r^{2\nu-2} R[\Phi_\nu] \right)^{3/2} = 0$$

where

$$\begin{aligned} P[\Phi_\nu] &= \Phi_\nu'' + \nu^2 \Phi_\nu \\ Q[\Phi_\nu] &= \nu^2 \Phi_\nu^2 \Phi_\nu'' + (\nu - \nu^2) \Phi_\nu (\Phi_\nu')^2 + \nu^3 \Phi_\nu^3 \\ R[\Phi_\nu] &= (\Phi_\nu')^2 + \nu^2 \Phi_\nu^2 \end{aligned}$$

Considering all possible values of ν , leaving only main terms in r (the smallest powers of r) and solving for $\Phi_\nu(\phi)$ in each case, one arrives at the following set of solutions (only even terms are shown due to the symmetry of the problem):

$$\Phi_\nu(\phi) = \begin{cases} C \cos^\nu \phi & \text{if } 0 < \nu < 1 \\ C \cos \phi & \text{if } \nu = 1 \\ C \cos \nu \phi & \text{if } 1 < \nu < 2 \\ C \cos 2\phi - \frac{1}{4} & \text{if } \nu = 2 \\ \text{no solution} & \text{if } \nu > 2 \end{cases}$$

(C is independent of r and ϕ everywhere but arbitrary otherwise.) Obviously, the first two options can not satisfy boundary conditions $\Phi_\nu(-\alpha/2) = \Phi_\nu(\alpha/2) = 0$ for angles $\alpha < \pi$, and thus the “not horizontal” solutions with $\nu \leq 1$ are naturally eliminated. In cases 3 and 4 boundary conditions yield $\nu = \pi/\alpha$ and $C = 1/(4 \cos \alpha)$ respectively. Thus, the main order result in the limit $r \ll 1$ is nothing but eq. (14):

$$z(r, \phi) = \begin{cases} \frac{1}{4} r^2 \left(\frac{\cos 2\phi}{\cos \alpha} - 1 \right) & \text{if } 0 \leq \alpha < \frac{\pi}{2} \quad (\nu = 2) \\ C r^{\pi/\alpha} \cos \frac{\pi \phi}{\alpha} & \text{if } \frac{\pi}{2} < \alpha \leq \pi \quad (\nu = \pi/\alpha) \end{cases}$$

Then we proceed in exactly the same fashion to determine μ and to find $\Phi_\mu(\phi)$ by employing just calculated main order result. Substitution of the first two terms of the expansion (13) into equation (1) yields the following equation for $\Phi_\mu(\phi)$:

$$\begin{aligned} r^\nu \left(P[\Phi_\nu] + r^{\mu-\nu} U[\Phi_\mu] + r^{2\nu-2} Q[\Phi_\nu] + r^{\nu+\mu-2} V[\Phi_\nu, \Phi_\mu] + O(r^{2\mu-2}) \right) + \\ + r^2 \left(1 + r^{2\nu-2} R[\Phi_\nu] + r^{\nu+\mu-2} W[\Phi_\nu, \Phi_\mu] + O(r^{2\mu-2}) \right)^{3/2} = 0 \end{aligned}$$

where $\Phi_\nu(\phi)$ is already known, P, Q, R are the same as in the equation for $\Phi_\nu(\phi)$,

$$U[\Phi_\mu] = \Phi_\mu'' + \mu^2 \Phi_\mu$$

and expressions for V and W are irrelevant to any final results. Similar to the previous case analysis, including thorough consideration of all possible cases for values of μ , neglect of the terms of the order higher than the first correction in r and application of symmetry arguments and boundary conditions to the solutions, leads to the first-order result (15)-(18).

Obviously, the procedure of building the next term of power series for the solution of eq. (1) can be repeated up to an arbitrary order.

References

- [1] R. Finn, *Equilibrium Capillary Surfaces* (Springer-Verlag, 1986).
- [2] L.D. Landau, E.M. Lifshitz, *Fluid Mechanics* (Course of Theoretical Physics, Volume 6), 2nd English edition, Section 61 (Pergamon Press, 1987).
- [3] A.D. Myshkis, V.G. Babskii, N.D. Kopachevskii, L.A. Slobozhanin, A.D. Tyuptsov, *Low-Gravity Fluid Mechanics*, Chapter 2 (Springer-Verlag, 1987).
- [4] I. Cohen, M.P. Brenner, J. Eggers, S.R. Nagel, *Phys. Rev. Lett.* **83**, 1147 (1999).
- [5] J. Eggers, *Rev. Mod. Phys.* **69**, 865 (1997).
- [6] M.P. Brenner, J.R. Lister, H.A. Stone, *Phys. Fluids* **8**, 2827 (1996).
- [7] Y.D. Shikmurzaev, *Phys. Fluids* **12**, 2386 (2000).
- [8] J. Eggers, J.R. Lister, H.A. Stone, *J. Fluid Mech.* **401**, 293 (1999).
- [9] J. Eggers, *Phys. Rev. Lett.* **80**, 2634 (1998).
- [10] P.G. de Gennes, *Rev. Mod. Phys.* **57**, 827 (1985).
- [11] G.F. Teletzke, H.T. Davis, L.E. Scriven, *Chem. Eng. Commun.* **55**, 41 (1987).
- [12] E.L. Decker, S. Garoff, *J. Adhesion* **63**, 159 (1997).
- [13] Y.D. Shikmurzaev, *J. Fluid Mech.* **334**, 211 (1997).
- [14] L. Mahadevan, Y. Pomeau, *Phys. Fluids* **11**, 2449 (1999).
- [15] M.O. Robbins, J.F. Joanny, *Europhys. Lett.* **3**, 729 (1987).
- [16] V.E.B. Dussan, *Annu. Rev. Fluid Mech.* **11**, 371 (1979).
- [17] V.E.B. Dussan, E. Rame, S. Garoff, *J. Fluid Mech.* **230**, 97 (1991).
- [18] A. Belmonte, *Pheol. Acta* **39**, 554 (2000).
- [19] R. Chhabra, D. de Kee, *Transport processes in bubbles, drops and particles* (Hemisphere Publishing, 1992).

- [20] R. Chhabra, *Bubbles, drops and particles in non-Newtonian fluids* (CRC Press, 1993).
- [21] R.D. Deegan, O. Bakajin, T.F. Dupont, G. Huber, S.R. Nagel, T.A. Witten, *Phys. Rev. E* **62**, 756 (2000).
- [22] R.D. Deegan, *Phys. Rev. E* **61**, 475 (2000).
- [23] R.D. Deegan, O. Bakajin, T.F. Dupont, G. Huber, S.R. Nagel, T.A. Witten, *Nature* **389**, 827 (1997).
- [24] G.A. Korn, T.M. Korn, *Mathematical Handbook For Scientists and Engineers*, Section 17.3 (McGraw-Hill, 1961).